

## EMULSIONS AS VEHICLES FOR THE CONTROLLED RELEASE OF ASTAXANTHIN IN TOPICAL APPLICATION

Michał Dymek\*, Elżbieta Sikora

Cracow University of Technology, Faculty of Chemical Engineering and Technology,  
Warszawska 24, 31-155 Kraków, Poland

In the work, the antioxidant activity of astaxanthin (AST) and the influence of the base formulation on the kinetics of AST release were studied. Three stable O/W AST-loaded emulsions, differing in droplet size (12.7  $\mu\text{m}$  (E1), 3.8  $\mu\text{m}$  (E2), 3.2  $\mu\text{m}$  (E3)) and a nanoemulsion (0.13  $\mu\text{m}$ , NE) were prepared. The results confirmed very strong antioxidant activity of AST. The emulsion internal phase droplet size did not significantly affect the AST release. The amount of released AST was respectively: 13.60% (E1), 11.42% (E2), 9.45% (E3), 9.71% (NE). The best fit to experimental data was obtained using the Higuchi model for emulsions and the Korsmeyer-Peppas model for NE. The results show that the AST release process is limited by the diffusion through carriers and the prepared O/W emulsions can be applied as vehicles for delivery of astaxanthin to the skin, ensuring effective anti-aging action of the cosmetics.

**Keywords:** astaxanthin, release kinetics, skin delivery systems, emulsions, antioxidant activity

### 1. INTRODUCTION

Modern cosmetics provide a comprehensive care for the skin owing to the content of different active ingredients. They show moisturizing, anti-wrinkle, anti-oxidant and anti-aging properties or protect skin against UV radiation. One such ingredient that is gaining popularity is astaxanthin (AST). AST is a hydrophobic, dark red substance, belonging to the xanthophyll group, found in nature in aquatic organisms, such as microalgae, shrimps, crabs and salmon, both in free and esterified form (Guerin et al., 2003; Higuera-Ciapara et al., 2006; Lorenz and Cysewski, 2000). On an industrial scale, it is obtained from *Haematococcus pluvialis* microalgae, which contains up to 3-5% of astaxanthin in dry matter (Chekanov et al., 2014). AST is obtained using supercritical CO<sub>2</sub> extraction of algae or from food industry waste materials, such as shrimp residues, which allows to obtain AST without the risk of its decomposition (Radzali et al., 2014; Reyes et al., 2014). The most important properties of astaxanthin, from the cosmetics point of view, are its strong free radical scavenging abilities related to the presence of conjugated double bonds in its molecule (Guerin et al., 2003). Its antioxidant activity is similar to that of butylhydroxyanisole, a synthetic cosmetic antioxidant ingredient (Sila et al., 2013). Compared to other carotenoids, such as

\* Corresponding author, e-mail: [michal.dymek@doktorant.pk.edu.pl](mailto:michal.dymek@doktorant.pk.edu.pl)

Reprinted with permission in an extended form from the EYEC Monograph accompanying 9th European Young Engineers Conference

<https://journals.pan.pl/cpe>



canthaxanthin or  $\beta$ -carotene, AST has a stronger antiradical activity, that is why it is popularly called the “queen of carotenoids” (Chang et al., 2013). Used as a cosmetic ingredient, astaxanthin protects skin against harmful UVA radiation, limiting transepidermal water loss (TEWL) and wrinkles (Komatsu et al., 2017). Also taken orally, AST reduces wrinkles (“crow’s feet”) and hyperpigmentation changes, increasing skin elasticity (Tominaga et al., 2012). Its protective effects against oxidative stress (Al-Bulish et al., 2017) and inflammation are also observed (Chew et al., 2013). Additionally, AST accelerates wound healing and prevents scab formation (Meehansan et al., 2017), and also protects against the development of burn wounds (Fang et al., 2017).

It is commonly known that the efficiency of cosmetics is related to the effective delivery of the active substance from the cosmetic to the skin and controlled release, i.e., ensuring a constant drug delivery over time, independent of the initial concentration (Lasoń et al., 2020). There are several reports in the literature studying the influence of the carrier (base formulation) on AST release. Lee et al. studied release of astaxanthin from nanoporous silicified-phospholipids assembled boron nitride complex (Lee et al., 2017). The effect of particle size on astaxanthin release from ethyl cellulose carriers was analyzed by Tirado and co-authors (Tirado et al., 2019). Shanmugapriya and co-authors tested combined O/W nanoemulsions, prepared by spontaneous or ultrasonic emulsification, as carriers of AST (Shanmugapriya et al., 2018). Stable over a wide temperature range complexes of AST with cyclodextrins were also described (Yuan et al., 2013).

However, there are still few studies dealing with the influence of carriers on the release of AST from different dermal delivery systems. The aim of the study was to determine the antioxidant properties of natural astaxanthin obtained by supercritical CO<sub>2</sub> extraction of *Haematococcus pluvialis* microalgae. Moreover, the influence of the droplet size and the polarity of the lipid phase of the emulsions on astaxanthin release was studied, various mathematical models were applied to describe the kinetics of astaxanthin transport.

## 2. MATERIALS AND METHODS

### 2.1. Materials

The supercritical CO<sub>2</sub> *Haematococcus pluvialis* microalgae extract containing astaxanthin (Algalif Astaxanthin 5%) was kindly supplied by Algalif (Iceland). HPLC grade astaxanthin standard was purchased from Sigma-Aldrich. The emulsion ingredients were of cosmetic grade. Crodamol GTCC, Natragem EW-FL, Tween 20, Tween 80 and Arlacel 2121 were kindly supplied by Croda, Poland. Borage and black cumin oil were purchased from Olvita sp. z o.o. Vitamin E was provided by DSM Nutritional Products. All other chemicals as potassium dihydrogen phosphate (POCh), sodium hydrogen phosphate (POCh), sodium persulfate (POCh) were of analytical grade. Deionised water, filtered through a Milli-Q system, was used for the aqueous phase of the emulsion.

### 2.2. Radical scavenging capacity assay

In order to determine the antioxidant properties, a modified ABTS (2,2'-azino-bis(3-ethylbenzothiazoline-6-sulfonic acid)) radical scavenging capacity assay (Re et al., 1999) was used. 7.4 mM aqueous solution of ABTS and 2.6 mM aqueous solution of Na<sub>2</sub>S<sub>2</sub>O<sub>8</sub> were mixed in a 1:1 volume ratio and stored at 8 °C for 12 hours in the dark. Next, 5.5 cm<sup>3</sup> of the solution was taken out and mixed with 60 cm<sup>3</sup> of ethanol. The antioxidant property assays were carried out for AST standard (chemically pure), for the AST containing extract (Algalif) and for vitamin E. An appropriate amount of each sample: AST standard and algae extract, containing approximately 0.001 g of AST, was mixed with 5 cm<sup>3</sup> of ethanol and then shaken

(Vortex) for 15 minutes. Additionally, the mixture of ethanol and 0.001 g of vitamin E was prepared in order to compare its antioxidant properties with the AST sample. Afterwards, 2.85 cm<sup>3</sup> of ABTS solution was mixed with 0.15 cm<sup>3</sup> of each of the test samples (ethanolic solutions containing AST or vitamin E) or 0.150 cm<sup>3</sup> of ethanol (as a reference sample). 2 hours after the initiation of the reaction with the radical for each of the mixtures, the absorbance measurements were performed using a NANOCOLOR UV-VIS spectrophotometer (Macherey-Nagel), at a wavelength of 734 nm. The degree of ABTS radical inhibition,  $I_{\%}$ , (ABTS scavenging ability) was calculated using Eq. (1):

$$I_{\%} = \frac{A_k - A_p}{A_k} \cdot 100\% \quad (1)$$

### 2.3. Surface tension of oils

For capric-caprylic triglycerides (O1) and a mixture (1:1, w/w) of borage and black cumin oils (O2), to estimate the oil polarity, the surface tension was measured by a tensiometric method. Measurements were carried out at a constant temperature of 25 °C, using a STA-1 Sinterface Technologies tensiometer equipped with a Du Nouy platinum ring system. The result was the average of 10 measurements.

### 2.4. Preparation of emulsions

As the cosmetic bases (astaxanthin carriers containing 0.1% wt. of AST) O/W emulsions differing in droplet sizes (E1, E2) or in applied oils (E3) as well as a nanoemulsion system (NE) were prepared. Additionally, as a reference sample (O1), Crodamol GTCC was used. The compositions of the obtained formulations are presented in Table 1. In order to prepare the formulations, the appropriate amount of water and emulsifier (Arlacel 2121) was placed into a beaker and dispersed using a magnetic stirrer (IKA C-MAG HS 7), at temperature  $T = 65$  °C.

Table 1. Composition of prepared formulations

Name of ingredients	INCI name of ingredients	Content [% wt.]			
		E1, E2	E3	NE	O1
Water	Aqua	76	76	80	–
Crodamol GTCC	Caprylic/Capric Triglyceride	15	–	2	98
Natragem EW-FL	Glyceryl Stearate (and) Polyglyceryl-6 Palmitate/Succinate (and) Cetearyl Alcohol	4.5	4.5	–	–
Arlacel 2121	Sorbitan Stearate (and) Sucrose Cocoate	2.5	2.5	-	-
Algalif Astaxanthin 5%	Helianthus Annuus Seed Oil (and) Astaxanthin	2	2	2	2
Borage oil	Borago Officinalis Seed Oil	–	7.5	–	–
Black cumin oil	Nigella Sativa Seed Oil	–	7.5	–	–
Tween 80	Polysorbate 80	–	–	16	–

Next, the ingredients of the oil phase: Natragem EW-FL, Algalif Astaxanthin 5% extract and, depending on the type of sample, Crodamol GTCC or a mixture of natural oils (black cumin and borage oils) were weighed in a separate beaker and mixed at the same temperature, as the water phase. In the next stage, both phases were mixed using a high shear homogenizer (CAT Unidrive X 1000) by pouring the water phase into the oil phase and homogenizing the mixture for 6 minutes. The E1 emulsion was homogenized at 3500 rpm, the E2 and E3 emulsions were homogenized at 11000 rpm. After preparation, all samples were stored at room temperature. NE was obtained by the phase inversion composition (PIC) method ([16]Jaworska et al., 2013). First, the active was dissolved in the oil/surfactant mixture. The appropriate amount of polysorbate 80, Crodamol GTCC and Algalif Astaxanthin 5% was weighed and shaken using Vortex shaker (IKA) for 15 minutes until a homogeneous mixture was obtained. Water was then added dropwise to the oil/surfactant/AST mixture while shaking continuously, until a clear/transparent formulation was obtained. O1 was prepared by dissolving a suitable amount of the algae extract in Crodamol GTCC, at 65 °C.

### 2.5. Particle size measurements and stability study

The average size of oil droplets in the emulsions (E1, E2, E3) was measured with an optical microscope, Motic B1, equipped with a digital camera and connected to a digital image processing software. One drop of each formulation was applied to a microscope slide, then covered with a coverslip to form a thin layer of the samples. The emulsion droplets were observed through an objective lens of 40X magnification. In the case of the nanoemulsion, the average size and size distribution of droplets were measured by means of dynamic light scattering method (DLS), using a particle size analyzer Malvern Zetasizer Nano-Z/S, at  $T = 25$  °C. For each sample, three replicates were performed. The stability of the formulations was studied by the centrifugal method and freeze/thaw stability (FTS) study (Sikora, 2019). Samples of the emulsions and nanoemulsion were placed in a heat dish of a centrifuge and spun at 3500 rpm for 10 minutes. Next, the formulations were visually inspected for any changes in their texture. During FTS test the emulsions and nanoemulsion were placed for 24 hours, at minus temperature ( $T < -10$  °C) followed by  $T = 40$  °C to determine the effect that freezing and subsequent thawing had upon the stability of the formulations. The studies were conducted with three cycles.

### 2.6. Study of rheological properties

The rheological measurements were carried out using a Brookfield Model R/S Plus rheometer equipped with a plate-cone system (C-25-2). Measurements were carried out three times for each formulation, in the shear rate range of  $1-500$  s<sup>-1</sup>, at 25 °C, for 50 seconds. Each time a 2 cm<sup>3</sup> sample of the formulation was placed on the measuring plate.

### 2.7. Release studies

AST release kinetics studies were carried out using Spectra/Por RC dialysis bags (MWCO; 6–8 kDa), at the temperature of 32 °C. Three repetitions were made for each of the samples. The dialysis bags were filled with about 3 g of the prepared formulations and placed in a thermostatic chamber filled with a solution (99.5/0.5; w/w) of phosphate buffer (PBS) of pH = 7.40 and polysorbate 20 – in order to increase the solubility of astaxanthin in hydrophilic acceptor solution (Chen et al., 2020). The concentration of released AST was determined with a Macherey-Nagel UV-vis spectrophotometer, at  $\lambda = 480$  nm, on the basis of the previously prepared calibration curve of absorbance,  $A$ , as a function of AST concentration,  $C_{AST}$  ( $A = 0.0086 \cdot C_{AST} - 0.0015$ ;  $R^2 > 0.999$ ). The analysis of the obtained results was made using linear regression for four models: zero and first order (Costa and Lobo, 2001), Higuchi (Dash et al., 2010;

Higuchi, 1961; Higuchi, 1963; Petropoulos et al., 2012) and Korsmeyer-Peppas (Dash et al., 2010; Peppas and Sahlin, 1989).

### 3. RESULTS AND DISCUSSION

#### 3.1. Radical scavenging capacity assay

The results of ABTS radical scavenging capacity assay are presented in Table 2.

Table 2. ABTS radical scavenging capacity assay results

Sample	ABTS scavenging ability [%]
AST standard	34.49
AST extract (Algalif)	99.74
Vitamin E	89.16

The data presented in Table 2 proved that SC-CO<sub>2</sub> *Haematococcus pluvialis* extract containing 5% of astaxanthin is characterized by very good antioxidant properties, stronger than vitamin E (89.16% of ABTS inhibition), deactivating the ABTS radical almost in 100%. Pure AST standard (Sigma-Aldrich) showed much weaker antioxidant properties. The clearly stronger radical scavenging effect of the AST containing extract than chemically pure substance may result from the synergistic effect of the astaxanthin and the other carotenoid esters present in the algae extract. The mixture of the actives eliminates free radicals more effectively (Régnier et al., 2015).

#### 3.2. Emulsion and oil characterization and stability

Three stable O/W AST-loaded emulsions and a nanoemulsion (Table 1) were prepared using different process parameters, as described in the experimental part, in order to obtain emulsions differing in droplet size of the internal phase (Table 4). The emulsions E1 and E2 had the same composition, in the case of the E3 the oil phase consisted of natural oils (borage and black cumin oils). In the case of the nanoemulsion (NE) and the E1 and E2 emulsions, caprylic/capric triglycerides (Crodamol GTCC) were used. As a reference sample, astaxanthin dissolved in capric/caprylic triglycerides was prepared. The oil surface tension measurement results are shown in Table 3.

Table 3. Surface tension of O1 and O2 oil phases

Oil mixture	Surface tension $\pm$ SD ( $n = 10$ ) [mN/m]
O1	23.96 $\pm$ 0.01
O2	29.27 $\pm$ 0.06

As the polarity of oils has a direct influence on their interfacial tension – the higher the interfacial tension, the lower the oil polarity (El-Mahrab-Robert et al., 2008), caprylic/capric triglycerides (O1) are more polar than the mixture of borage and black cumin oils (O2).

Optical micrographs of the emulsions (Fig. 1) revealed, as expected, that E2 emulsion, prepared with high-shear homogenization (11000 rpm), was a dispersion with droplets considerably smaller than those of E1 emulsion, which was obtained by lower-shear homogenization (3900 rpm). In emulsion E1, the low-shear homogenization process affected the irregular shape of droplets. The mean droplet size of E1, E2 and E3, calculated from a population of 600 droplets, was 12.7, 3.8 and 3.2  $\mu\text{m}$  respectively. The average droplet size of the nanoemulsion was determined with dynamic light scattering (DLS, Table 4).

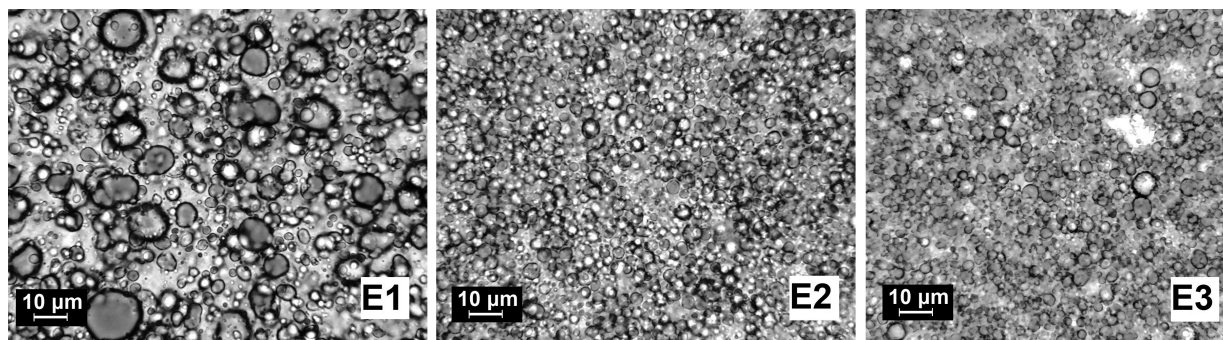


Fig. 1. Microscopic photos of E1, E2, E3 emulsions

Table 4. Droplet sizes of the prepared formulations

Formulation	Homogenizer rotational speed [rpm]	Mean diameter $\pm$ SD ( $n = 600$ ) [ $\mu\text{m}$ ]
E1	3900	$12.7 \pm 3.1$
E2	11000	$3.8 \pm 1.0$
E3	11000	$3.2 \pm 1.0$
NE	–	0.130 (PDI = 0.276)

The data presented in Table 4 revealed that the use of higher homogenizer rotation frequencies resulted in a decrease in the mean droplet diameter of the emulsion internal phase. Consequently, it is possible to obtain formulations with more uniform droplet sizes (lower SD), which may additionally increase their stability (Okonogi and Riangjanapatee, 2015). No significant difference was observed between the average droplet diameter of the emulsions containing oil phases of different polarity. DLS studies confirmed that the NE complied with the requirements (Aboofazeli, 2010) for nanometric scale cosmetic products ( $d = 0.130 \mu\text{m}$ ), and was also characterized by a low value of the polydispersity index (PDI = 0.276).

To sum up, the values of droplet size were considered sufficiently different to detect a possible effect of droplet size on AST release. Concerning stability, the formulations remained practically unchanged after the centrifugal tests and FTS study. The obtained results indicate that the formulations and the procedure used to prepare them were appropriate for skin permeation studies.

In the next stage of the research the rheological properties were established for the prepared AST-loaded formulations (Fig. 2).

All of the prepared formulations were non-Newtonian, shear thinning fluids. The parameters of homogenization process influence sample viscosity, with an increase of rotation frequencies the product viscosity also increases. For example, at the shear rate of  $100 \text{ s}^{-1}$ , the viscosity of E1 emulsion was 1100 mPa s while in the case of E2 – 1700 mPa s.

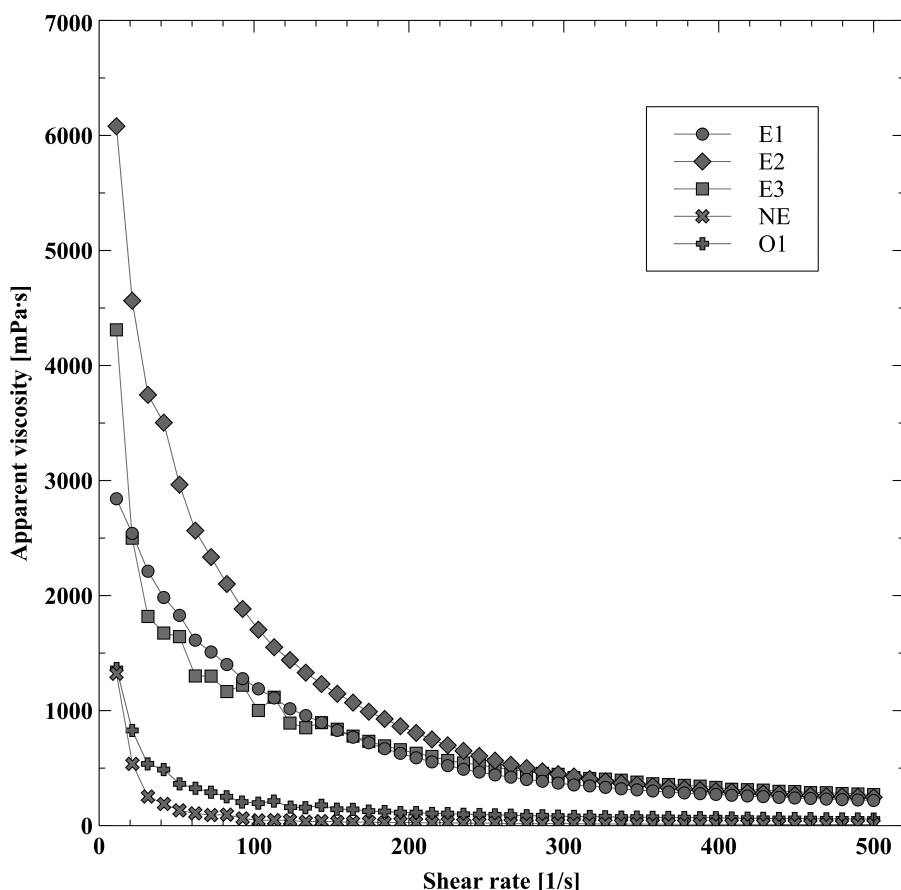


Fig. 2. Viscosity curves of the prepared formulations ( $T = 25\text{ }^{\circ}\text{C}$ )

### 3.3. AST release studies

The in vitro release profiles of astaxanthin from the prepared emulsions (E1, E2, E3), nanoemulsion (NE) and the oil phase (O1) as the control sample are shown in Fig. 3. The amount of the active ingredient in all studied carriers was 0.1% wt. As observed, the obtained profiles were similar and no significant differences in the percentage of the active release at 24 h were detected between formulations ( $13.60 \pm 0.95\%$ ,  $11.42 \pm 0.75\%$ ,  $9.46 \pm 0.36\%$ ,  $9.80 \pm 0.13\%$ ,  $7.68 \pm 0.15\%$  for E1, E2, E3, NE, O1, respectively). These differences are not significant from the cosmetic point of view.

The obtained results indicate that the droplet size of the emulsions does not influence the astaxanthin release from the carriers. This is confirmed even in the case of NE, despite the lowest droplet size of the internal phase ( $0.130\text{ }\mu\text{m}$ ), after 24 hours the released amount of AST was only slightly smaller than that of emulsions ( $d_{E1} = 12.7\text{ }\mu\text{m} \pm 3.1\text{ }\mu\text{m}$ ,  $d_{E2} = 3.8\text{ }\mu\text{m} \pm 1.0\text{ }\mu\text{m}$ ,  $d_{E3} = 3.2\text{ }\mu\text{m} \pm 1.0\text{ }\mu\text{m}$ ). On the other hand, comparing the amount of astaxanthin released from the E2 and E3 emulsions, similar in internal droplets size but differing in polarity of oil phase ( $23.96 \pm 0.01$  and  $29.27 \pm 0.06\text{ mN/m}$  for O1 and O2 respectively), we can conclude that the higher release rate of AST is related to the higher polarity of hydrophobic substances (Sikora et al., 2015), as the oil phase of E2 (caprylic/capric triglycerides, O1) is more polar than the oil phase of E3 emulsion (the mixture of borage and black cumin oils, O2). The lowest amount of AST ( $7.68\% \pm 0.15\%$ wt.) was released from the oil (O1). In the case of the reference sample we can explain it by a much higher affinity of AST to capric-caprylic triglycerides. However, the absence of significant differences observed between astaxanthin release from the prepared formulations could be explained by a residence of the actives at the lipid phase and/or at the lipid-rich interface (Izquierdo et al., 2007; Sikora et al., 2015).

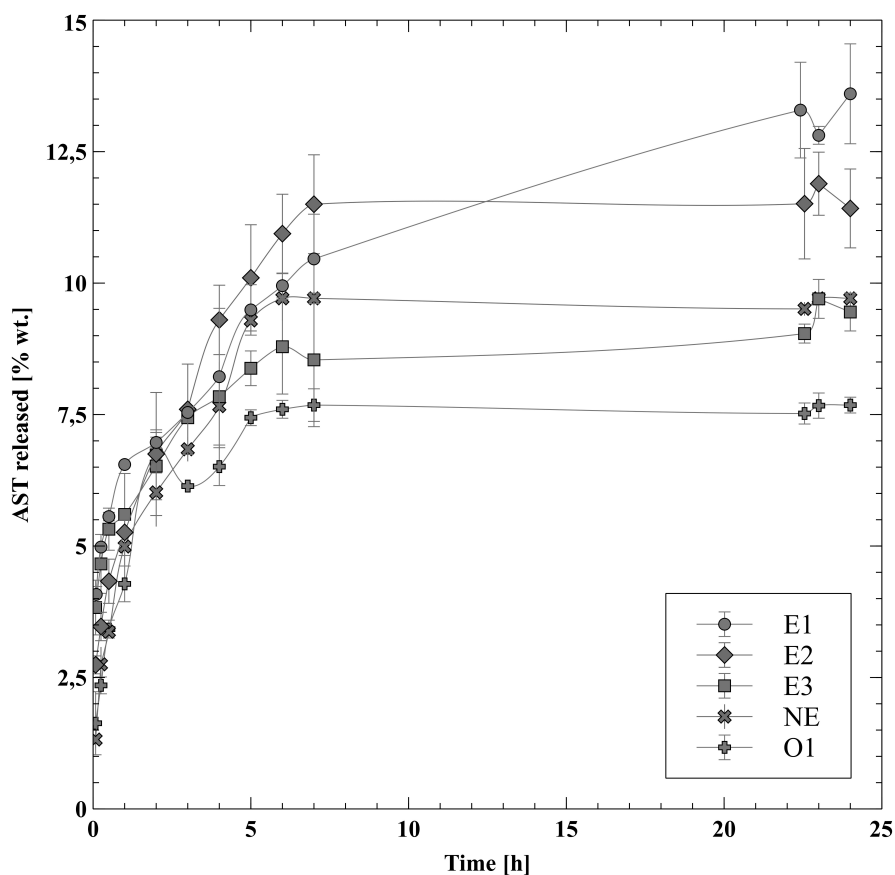


Fig. 3. Release profiles of astaxanthin from the nanoemulsion (NE), O/W emulsions (E1, E2, E3) and oil solution (O1)

In order to better understand the mechanism of AST release from the prepared carriers, a mathematical analysis was performed by fitting the most appropriate kinetic model. As in consumer conditions it is rare to keep an applied cosmetic for 24 hours on the surface of the skin, the calculations were made for the first 7 hours of the experiment, which was considered optimal. Among many mathematical models, the zero (Eq. (2)) and first order (Eq. (3)), Higuchi (Eq. (4)) and Korsmeyer-Peppas (Eq. (5)) models were selected to describe the release process. Systems with a constant mass exchange surface with an acceptor solution, for substances that are poorly soluble in water and penetrate not very quickly, usually show a good fit with the zero-order model. Moreover, it proves that the concentration of the active ingredient is kept constant, in contrast to the first-order model (Costa and Lobo, 2001). Higuchi's model is based on Fick's first law and is used in the description of the kinetics of release from emulsions and ointments, where the process is limited by the diffusion of the substance through the carrier, and the release itself is rather fast (Dash et al., 2010; Higuchi, 1961; Higuchi, 1963; Petropoulos et al., 2012). The Korsmeyer-Peppas model is an exponential model of release kinetics, used mainly to describe the behavior of pharmaceutical systems, in which the physical interpretation of the mechanism is related to the value of the  $n$  parameter appearing in the equation (Dash et al., 2010; Peppas and Sahlin, 1989). Although the Korsmeyer-Peppas model was originally developed for polymer matrices, it is now often used to describe pharmaceutical emulsion formulations (Olejnik et al., 2017). The applicability of this model is due to the similarities between the spherical matrices and the dispersed phase of stable emulsions.

$$\frac{M}{M_0} = K_0 \cdot t \quad (2)$$

$$\ln \frac{M}{M_0} = K_1 \cdot t \quad (3)$$

$$\frac{M}{M_0} = K_H \cdot t^{0.5} \tag{4}$$

$$\frac{M}{M_0} = K_{KP} \cdot t^n \tag{5}$$

The kinetic model parameters for the release results are shown in Table 5.

Table 5. The kinetic model parameters for the release results

Kinetic model	Parameter	Formulation				
		E1	E2	E3	NE	O1
Zero-order	R <sup>2</sup>	0.9541	0.9663	0.8995	0.9173	0.7957
	K <sub>0</sub> · 10 <sup>3</sup> [h <sup>-1</sup> ]	8.40	1.24	6.60	1.15	8.10
First-order	R <sup>2</sup>	0.8903	0.8772	0.8381	0.7355	0.7957
	K <sub>1</sub> · 10 <sup>1</sup> [h <sup>-1</sup> ]	1.17	1.88	1.04	2.23	1.80
Higuchi	R <sup>2</sup>	0.9798	0.9960	0.9782	0.9833	0.9164
	K <sub>H</sub> · 10 <sup>2</sup> [h <sup>-0.5</sup> ]	2.55	3.77	2.07	3.55	2.58
Korsmeyer-Peppas	R <sup>2</sup>	0.9710	0.9839	0.9854	0.9848	0.9698
	K <sub>KP</sub> · 10 <sup>2</sup> [h <sup>-n</sup> ]	6.49	5.68	6.00	4.45	4.17
	n	0.210	0.334	0.190	0.433	0.360

According to the results presented in the Table 5, the best fit of AST release from E1, E2, E3 emulsions and the O1 oil phase of the emulsion was obtained for the Higuchi model. Although for the E3 and O1 formulations a slightly better fit was achieved by the Korsmeyer-Peppas model, the values of the characteristic exponent *n* were much lower than the value of 0.43 (0.190 and 0.360, respectively). Moreover, the oil phase does not contain the active ingredient encapsulated in spherical carriers. Due to this fact they do not fit into the original assumptions of this model (Ritger and Peppas, 1987) and therefore the description of the release mechanism from E3 and O1 carriers by Korsmeyer-Peppas model was abandoned. A good fit with the Higuchi model for emulsion formulations (R<sup>2</sup> > 0.978) proves that the AST release process is controlled by diffusion through the carrier. This relationship may also explain the lack of correlation between the greater dispersion of the internal phase of the emulsion and the greater degree of AST release. The lower viscosity of E1 (1189 mPa·s) than that of E2 (1703 mPa·s) seems to have a major influence on the transport of the active ingredient. Smaller droplets provided a larger mass exchange surface (E2, E3), but the higher rotational frequencies of the homogenizer needed to achieve desirable droplet sizes also increased the matrix viscosity, which made it difficult for them to migrate to the mass transfer boundary layer, which is the cellulose membrane. It can therefore be assumed that in this case the matrix - acceptor solution penetration is fast, and the whole process is controlled by diffusion through the carrier, so the formulations with lower viscosities and larger droplet sizes (E1) achieve higher AST release rates. NE can best be described using the Korsmeyer-Peppas model (R<sup>2</sup> > 0.98). The obtained value of the *n* parameter (*n* = 0.433) for it is very close to the characteristic value of 0.43 in this model for particles of spherical shape (Ritger and Peppas, 1987), which proves that the mechanism of AST release from NE is related to the classic Fickian diffusion. At the same time, the good fit with the zero-order model for O/W emulsions (R<sup>2</sup> > 0.95) indicates that it was possible to obtain carriers providing a constant concentration of the active ingredient in the skin and the possibility of controlled release of AST. The results are consistent with the data provided by Lee and co-authors (Lee et al., 2017) for AST encapsulated in tetraethyl orthosilicate modified liposomes, where the release process was controlled by its diffusion through the carrier and fits the zero-order model.

#### 4. CONCLUSIONS

In the study, astaxanthin obtained by SC-CO<sub>2</sub> extraction of the *Haematococcus pluvialis* microalgae was used. The free radical scavenging capacity assay confirmed that the actives showed very good antioxidant properties, inactivating the ABTS radical in almost 100%.

Three AST-loaded, kinetically stable, O/W emulsions, two with the same composition and different droplet size (12.7 μm (E1), 3.8 μm (E2)) and one differing in oil phase composition but with similar droplet size (3.2 μm (E3)) were obtained. Moreover, a nanoemulsion (0.13 μm) and an oil solution, containing AST, at the same concentration of 0.1% w/w, were prepared. The results of release studies showed that the emulsion droplet size did not significantly affect the amount of released AST, which for the prepared formulations was respectively: 13.60% (E1), 11.42% (E2), 9.45% (E3), 9.71% (NE) and that the oil phase polarity also slightly influenced the release of AST. Kinetic evaluation of release profiles was determined by fitting the experimental data to mathematical models describing different kinetic orders. The obtained results showed that the process of AST release from the O/W emulsions is limited by diffusion through the carrier, which is probably directly related to the viscosity of the medium. For the emulsion, the best fit of experimental data was achieved for the Higuchi model, while for the nanoemulsion – the Korsmeyer–Peppas model fits well the experimental data.

To sum up, the obtained results confirm that the prepared emulsion systems are suitable carriers for astaxanthin delivery. Combined with AST excellent antioxidant properties, the elaborated formulations can be applied in modern deeply caring and anti-aging cosmetics.

#### SYMBOLS

$I_{\%}$	the degree of ABTS radical inhibition, %
$A_k$	absorbance of the reference sample
$A_p$	absorbance of the test sample
$A$	absorbance of a sample
$C_{AST}$	AST concentration, mg/cm <sup>3</sup>
$d$	mean diameter of the internal phase droplets, μm
$M$	mass of released AST, mg
$M_0$	initial AST mass in the carrier, mg
$t$	time, h
$n$	exponent characteristic for specific diffusion mechanisms
$K_0$	constant for the zero-order kinetics model, h <sup>-1</sup>
$K_1$	constant for the first order kinetics model, h <sup>-1</sup>
$K_H$	constant for the Higuchi model, h <sup>-0.5</sup>
$K_{KP}$	constant for the Korsmeyer-Peppas model, h <sup>-n</sup>

#### Greek symbols

$\lambda$	wavelength, nm
-----------	----------------

#### ACKNOWLEDGEMENTS

Special acknowledgements to Dr. Haraldur Gardarsson and Algalif Iceland ehf. for providing free samples of the astaxanthin extract, without which the presented research would not have been possible.

## REFERENCES

- Aboofazeli R., 2010. Nanometric-scaled emulsions (nanoemulsions). *Iran. J. Pharm. Res.*, 9, 4, 325–326.
- Al-Bulish M.S.M., Xue C., Waly M.I., Xu J., Wang Y., Tang Q.-J., 2017. The defensive role of antioxidants astaxanthin against oxidative damage in diabetic rats injected with streptozotocin. *J. Food Nutr. Res.*, 5, 191–196. DOI: [10.12691/jfnr-5-3-9](https://doi.org/10.12691/jfnr-5-3-9).
- Chang C-S., Chang C-L., Lai G-H., 2013. Reactive oxygen species scavenging activities in a chemiluminescence model and neuroprotection in rat pheochromocytoma cells by astaxanthin, beta-carotene and canthaxanthin. *Kaohsiung J. Med. Sci.*, 29, 412–421. DOI: [10.1016/j.kjms.2012.12.002](https://doi.org/10.1016/j.kjms.2012.12.002).
- Chekanov K., Lobakova E., Selyakh I., Semenova L., Sidorov R., Solovchenko A., 2014. Accumulation of astaxanthin by a new *Haematococcus pluvialis* strain BM1 from the white sea coastal rocks (Russia). *Mar Drugs*, 12, 4504–4520. DOI: [10.3390/md12084504](https://doi.org/10.3390/md12084504).
- Chen Z., Li W., Shi L., Jiang L., Li M., Zhang C., Peng H., 2020. Kidney-targeted astaxanthin natural antioxidant nanosystem for diabetic nephropathy therapy. *Eur. J. Pharm. Biopharm.*, 156, 143–154. DOI: [10.1016/j.ejpb.2020.09.005](https://doi.org/10.1016/j.ejpb.2020.09.005).
- Chew W., Mathison B., Kimble L., Mixer P.F., Chew B.P., 2013. Astaxanthin decreases inflammatory biomarkers associated with cardiovascular disease in human umbilical vein endothelial cells. *Am. J. Food Technol.*, 1, 1–17. DOI: [10.7726/ajafst.2013.1001](https://doi.org/10.7726/ajafst.2013.1001).
- Costa P., Lobo J.M.S., 2001. Modeling and comparison of dissolution profiles. *Eur. J. Pharm. Sci.*, 13, 123–133. DOI: [10.1016/s0928-0987\(01\)00095-1](https://doi.org/10.1016/s0928-0987(01)00095-1).
- Dash S., Murthy P.N., Nath L., Chowdhury P., 2010. Kinetic modeling on drug release from controlled drug delivery systems. *Acta Pol. Pharm.*, 67, 3, 217–223.
- El-Mahrab-Robert M., Rosilio V., Bolzinger M.A., Chaminade P., Grossiord J.L., 2008. Assessment of oil polarity: Comparison of evaluation methods. *Int. J. Pharm.*, 348, 89–94. DOI: [10.1016/j.ijpharm.2007.07.027](https://doi.org/10.1016/j.ijpharm.2007.07.027).
- Fang Q., Guo S., Zhou H., Han R., Wu P., Han C., 2017. Astaxanthin protects against early burn-wound progression in rats by attenuating oxidative stress-induced inflammation and mitochondria-related apoptosis. *Sci. Rep.*, 7, 41440. DOI: [10.1038/srep41440](https://doi.org/10.1038/srep41440).
- Guerin M., Huntley M.E., Olaizola M., 2003. *Haematococcus* astaxanthin: applications for human health and nutrition. *Trends Biotechnol.*, 21, 210–216. DOI: [10.1016/S0167-7799\(03\)00078-7](https://doi.org/10.1016/S0167-7799(03)00078-7).
- Higuchi T., 1961. Rate of release of medicaments from ointment bases containing drugs in suspension. *J. Pharm. Sci.*, 50, 874–875. DOI: [10.1002/jps.2600501018](https://doi.org/10.1002/jps.2600501018).
- Higuchi T., 1963. Mechanism of sustained-action medication. Theoretical analysis of rate of release of solid drugs dispersed in solid matrices. *J. Pharm. Sci.*, 52, 1145–1149. DOI: [10.1002/jps.2600521210](https://doi.org/10.1002/jps.2600521210).
- Higuera-Ciapara I., Félix-Valenzuela L., Goycoolea F.M., 2006. Astaxanthin: A review of its chemistry and applications. *Crit. Rev. Food Sci. Nutr.*, 46, 185–196. DOI: [10.1080/10408690590957188](https://doi.org/10.1080/10408690590957188).
- Izquierdo P., Wiechers J.W., Escribano E., García-Celma M.J., Tadros T.F., Esquena J., Dederén J.C., Solans C., 2007. A study on the influence of emulsion droplet size on the skin penetration of tetracaine. *Skin Pharmacol. Physiol.*, 20, 263–270. DOI: [10.1159/000106076](https://doi.org/10.1159/000106076).
- Jaworska M., Sikora E., Zielina M., Ogonowski J., 2013. Studies on the formation of O/W nano-emulsions, by low-energy emulsification method, suitable for cosmeceutical applications. *Acta Biochim. Pol.*, 60, 779–782. DOI: [10.18388/abp.2013\\_2057](https://doi.org/10.18388/abp.2013_2057).
- Komatsu T., Sasaki S., Manabe Y., Hirata T., Sugawara T., 2017. Preventive effect of dietary astaxanthin on UVA-induced skin photoaging in hairless mice. *PLoS ONE*, 12, e0171178. DOI: [10.1371/journal.pone.0171178](https://doi.org/10.1371/journal.pone.0171178).
- Lasoń E., 2020. Sub-micron vehicles of biologically active substances, In: Sikora E., Miastkowska M., Lasoń E. (Eds.), *Selected skin delivery systems*. Wydawnictwo PK, Kraków, 80–109.
- Lee H.S., Sung D.K., Kim S.H., Choi W.I., Hwang E.T., Choi D.J., Chang J.H., 2017. Controlled release of astaxanthin from nanoporous silicified-phospholipids assembled boron nitride complex for cosmetic applications. *Appl. Surf. Sci.*, 424, 15–19. DOI: [10.1016/j.apsusc.2017.03.036](https://doi.org/10.1016/j.apsusc.2017.03.036).

- Lorenz R.T., Cysewski G.R., 2000. Commercial potential for *Haematococcus* microalgae as a natural source of astaxanthin. *Trends Biotechnol.*, 18, 160–167. DOI: [10.1016/s0167-7799\(00\)01433-5](https://doi.org/10.1016/s0167-7799(00)01433-5).
- Meehansan J., Rungjang A., Yingmema W., Deenonpoe R., Ponnikorn S., 2017. Effect of astaxanthin on cutaneous wound healing. *Clin. Cosmet. Invest. Dermatol.*, 10, 259–265. DOI: [10.2147/CCID.S142795](https://doi.org/10.2147/CCID.S142795).
- Okonogi S., Riangjanapatee P., 2015. Physicochemical characterization of lycopene-loaded nanostructured lipid carrier formulations for topical administration. *Int. J. Pharm.*, 478, 726–735. DOI: [10.1016/j.ijpharm.2014.12.002](https://doi.org/10.1016/j.ijpharm.2014.12.002).
- Olejnik A., Kapuscinska A., Schroeder G., Nowak I., 2017. Physico-chemical characterization of formulations containing endomorphin-2 derivatives. *Amino Acids*, 49, 1719–1731. DOI: [10.1007/s00726-017-2470-x](https://doi.org/10.1007/s00726-017-2470-x).
- Peppas N.A., Sahlin J.J., 1989. A simple equation for the description of solute release. III. Coupling of diffusion and relaxation. *Int. J. Pharm.*, 57, 169–172. DOI: [10.1016/0378-5173\(89\)90306-2](https://doi.org/10.1016/0378-5173(89)90306-2).
- Petropoulos J.H., Papadokostaki K.G., Sanopoulou M., 2012. Higuchi's equation and beyond: Overview of the formulation and application of a generalized model of drug release from polymeric matrices. *Int. J. Pharm.*, 437, 178–191. DOI: [10.1016/j.ijpharm.2012.08.012](https://doi.org/10.1016/j.ijpharm.2012.08.012).
- Radzali S.A., Baharin B.S., Othman R., Markom M., Rahman R.A., 2014. Co-solvent selection for supercritical fluid extraction of astaxanthin and other carotenoids from *Penaeus monodon* waste. *J. Oleo Sci.*, 63, 769–777. DOI: [10.5650/jos.ess13184](https://doi.org/10.5650/jos.ess13184).
- Re R., Pellegrini N., Proteggente A., Pannala A., Yang M., Rice-Evans C., 1999. Antioxidant activity applying an improved ABTS radical cation decolorization assay. *Free Radical Biol. Med.*, 26, 1231–1237. DOI: [10.1016/s0891-5849\(98\)00315-3](https://doi.org/10.1016/s0891-5849(98)00315-3).
- Régnier P., Bastias J., Rodriguez-Ruiz V., Caballero-Casero N., Caballo C., Sicilia D., Fuentes A., Maire M., Crepin M., Letourneur D., Gueguen V., Rubio S., Pavon-Djavid G., 2015. Astaxanthin from *Haematococcus pluvialis* prevents oxidative stress on human endothelial cells without toxicity. *Mar. Drugs*, 13, 2857–2874. DOI: [10.3390/md13052857](https://doi.org/10.3390/md13052857).
- Reyes F.A., Mendiola J.A., Ibañez E., del Valle J.M., 2014. Astaxanthin extraction from *Haematococcus pluvialis* using CO<sub>2</sub>-expanded ethanol. *J. Supercrit. Fluids*, 92, 75–83. DOI: [10.1016/j.supflu.2014.05.013](https://doi.org/10.1016/j.supflu.2014.05.013).
- Ritger P.L., Peppas N., 1987. A simple equation for description of solute release I. Fickian and non-fickian release from non-swelling devices in the form of slabs, spheres, cylinders or discs. *J. Controlled Release*, 5, 23–36. DOI: [10.1016/0168-3659\(87\)90034-4](https://doi.org/10.1016/0168-3659(87)90034-4).
- Shanmugapriya K., Kim H., Saravana P.S., Chun B.S., Kang H.W., 2018. Astaxanthin- $\alpha$ -tocopherol nanoemulsion formulation by emulsification methods: Investigation on anticancer, wound healing, and antibacterial effects. *Colloids Surf., B*, 172, 170–179. DOI: [10.1016/j.colsurfb.2018.08.042](https://doi.org/10.1016/j.colsurfb.2018.08.042).
- Sikora E., 2019. *Cosmetic emulsions*. Wydawnictwo PK, Kraków, 35–36.
- Sikora E., Llinas M., Garcia-Celma M.J., Escribano E., Solans C., 2015. Transdermal delivery of forskolin from emulsions differing in droplet size. *Colloids Surf., B*, 126, 541–545. DOI: [10.1016/j.colsurfb.2015.01.008](https://doi.org/10.1016/j.colsurfb.2015.01.008).
- Sila A., Ayed-Ajmi Y., Sayari N., Nasri M., Martinez-Alvarez O., Bougatef A., 2013. Antioxidant and anti-proliferative activities of astaxanthin extracted from the shell waste of deep-water pink shrimp (*Parapenaeus longirostris*). *Nat. Prod. J.*, 3, 82–89. DOI: [10.2174/2210315511303020002](https://doi.org/10.2174/2210315511303020002).
- Tirado D.F., Palazzo I., Scognamiglio M., Calvo L., Porta G.D., Reverchon E., 2019. Astaxanthin encapsulation in ethyl cellulose carriers by continuous supercritical emulsions extraction: A study on particle size, encapsulation efficiency, release profile and antioxidant activity. *J. Supercrit. Fluids*, 150, 128–136. DOI: [10.1016/j.supflu.2019.04.017](https://doi.org/10.1016/j.supflu.2019.04.017).
- Tominaga K., Hongo N., Karato M., Yamashita E., 2012. Cosmetic benefits of astaxanthin on humans subjects. *Acta Biochim. Pol.*, 59, 43–47. DOI: [10.18388/abp.2012\\_2168](https://doi.org/10.18388/abp.2012_2168).
- Yuan C., Du L., Jin Z., Xu X., 2013. Storage stability and antioxidant activity of complex of astaxanthin with hydroxypropyl- $\beta$ -cyclodextrin. *Carbohydr. Polym.*, 91, 385–389. DOI: [10.1016/j.carbpol.2012.08.059](https://doi.org/10.1016/j.carbpol.2012.08.059).

Received 30 May 2021

Received in revised form 20 September 2021

Accepted 11 October 2021